now published in J. Am. Chem. Soc., 127, 10699-10706 (2005)

Can the π–facial selectivity of solvation be predicted by atomistic simulation?

Roberto Berardi[A], Gianfranco Cainelli[B*], Paola Galletti[B], Daria Giacomini[B], Andrea Gualandi[B], Luca Muccioli[A], and Claudio Zannoni[A*].

Dipartimento di Chimica Fisica e Inorganica and INSTM, Università di Bologna, Viale Risorgimento 4, 40136 Bologna, Italy, and Dipartimento di Chimica "G. Ciamician", Università di Bologna, Via Selmi 2, 40126 Bologna, Italy.

*Claudio.Zannoni@unibo.it, *Gianfranco.Cainelli@unibo.it

ABSTRACT: This work is concerned with the rationalization and prediction of solvent and temperature effects in nucleophilic addition to α-chiral carbonyl compounds leading to facial diastereoselectivity. We study, using Molecular Dynamics simulations, the facial solvation of (*R*)-2-phenyl-propionaldehyde in *n*-pentane and *n*-octane at a number of temperatures and compare it with experimental selectivity data for the *n*BuLi addition leading to *syn* and *anti* (2*R*)-2-phenyl-3-heptanol, which give non-linear Eyring plots with the presence of inversion temperatures. We have found from simulations that the facial solvation changes with temperature and alkane. Moreover, by introducing a suitable molecular chirality index we have been able to predict break temperatures (T_{CI}) for the two solvents within less than 20 degrees of the inversion temperatures experimentally observed in the diastereoselective *n*BuLi addition. We believe this could lead to a viable approach for predicting inversion temperatures and other subtle solvent effects in a number of stereoselective reactions.

INTRODUCTION

It is well known that a number of chemical reactions can be affected by the medium in which the reaction takes place and that solvents can change both equilibrium constants and reaction rates [1]. The effects of solvent on stereoselectivity have already been well described by organic chemists, and in particular several examples of solvent dependent face-selectivity have been discussed [2]. However, a proper rationalization of these effects, and even more the possibility of predicting them from just knowledge of the compounds involved, is far from being in sight. To date, the two most common qualitative models employed to rationalize the reaction products of nucleophilic addition to α-chiral carbonyls are based on two arguments that actually disregard the effect of the solvent, assuming that the attack comes from the less sterically hindered direction, and that every aldehyde is at the same, fixed conformation. These are the Cram's model [3], predicting for this aldehyde a unique conformation in which the double bond is flanked by the two smallest groups (H, CH_3) attached to the chiral center, and the most successful Felkin–Ahn model [4,5], which instead predicts in this simple case the double bond to be flanked by the medium size group (CH_3) and lying between the two bulkiest groups (CH_3, Ph).

At a very simple level, the stereoselectivity is related, through the modified Eyring equation [6], to the difference $\Delta\Delta G^{\neq}$ on the free activation energies for the *syn* and *anti* reaction pathways leading to the two diastereoisomers,

$$\ln S(T) = \ln(k/k') = -\Delta\Delta G^{\neq}(T)/RT = -\Delta\Delta H(T)^{\neq}/RT + \Delta\Delta S(T)^{\neq}/R, \quad (1)$$

where S = [*anti*]/ [*syn*] is the stereoselectivity and k and k' are the overall rate constants for the synthesis of the two stereoisomers. Many experimental results show a non-linear temperature dependence for the selectivity, and a plot of ln$S$ vs. $1/T$ often consists of two straight lines with different slopes (corresponding to different activation parameters), intersecting at a temperature called the inversion temperature (T_{inv}) [7]. Here we are particularly interested in the role of the solvent in facial diastereoselectivity of α-chiral imines and carbonyl compounds, a case for which some of us have reported several interesting temperature dependence of the diastereomeric excess (de%) of the products

in polar and nonpolar solvents. For the model reaction involving addition of BuLi to 2-phenyl-propionaldehyde (scheme 1), the effect has been studied over a wide range of temperatures for various common organic solvents (*n*-pentane, *n*-hexane, cyclopentane, *n*-octane, *n*-decane, *n*-dodecane, cyclohexane, THF, tBuOMe, 1,4-dioxane) [8]. While the ethers show a linear dependence of de% on the temperature, all the alkanes present a break point at a certain temperature T_{inv}. In particular, for linear alkanes it has been observed that: (i) the *anti* product is favored at all temperatures; (ii) the selectivity decreases with the increase of temperature; (iii) the longer the solvent chain, the lower the diasterofacial selectivity; (iv) the inversion temperature correlates with the melting point of the alkane.

These facts are not easy either to rationalize intuitively or to be predicted by using quantum modelling [9], not only in the traditional "one molecule in vacuum approach", but also using fixed conformation continuum or discrete models with a few explicit solvent molecules to account for the solvent effect [10,11]. Indeed on one hand important differences in inversion temperatures are found in different linear alkanes with essentially the same dielectric constant and, on the other, the good conformational sampling in an equilibrium condensed phase that would be necessary to undertake the task is beyond the current possibilities of quantum chemical calculations.

The interpretative model that some of us have previously proposed is based on solvation effects [12]. Some examples have been reported for enantio- or diastereoselective reactions, where different reaction solvents are able to drive the diastereofacial selectivity [13]; the solvent plays a fundamental role as only small differences in activation enthalpies of the two diastereomeric transition states are expected. The presence of a T_{inv} would thus depend on dynamic solvation effects and represents the interconversion temperature of two different solvation clusters which act as two different supramolecules with different stereoselectivities. The dynamic solvent effects have been confirmed by temperature dependent studies of the ^{13}C NMR, CD and UV spectra of some solvated aldehydes in the absence of any reaction, revealing the presence of peculiar temperatures T_{CD}, T_{UV}, and T_{NMR}, whose values are identical and match with experimentally found T_{inv} [14], thus supporting its solvent-dependent nature.

To confirm this interpretation and establish its microscopical origin as well as to try to develop a predictive approach, we have decided to study the solvation of (*R*)-2-phenyl propionaldehyde in two solvents at first glance very similar: *n*-pentane and *n*-octane. The present paper is divided into two parts. In the first we investigate the experimental temperature-dependent diastereofacial selectivity in the addition reaction of *n*-BuLi to (*R*)-2-phenyl propionaldehyde: while data for the racemic aldehyde were already available [8], here we have obtained experimental data for the (*R*) enantiomer in *n*-pentane and in *n*-octane in a wide range of temperatures. In the second part we study, with the help of the molecular dynamics (MD) technique[15, 16], the temperature dependence of diastereosolvation in *n*-pentane and *n*-octane and we introduce some tools for following the change in solvation and, to some extent, to predict the inversion temperature.

EXPERIMENTAL PART

Optically pure (*R*)-2-phenyl propionaldehyde was prepared accordingly to the procedure reported in the literature by means of oxidation of (*R*)-2-phenyl-propanol with the Dess-Martin periodinane [17] (see scheme 1).

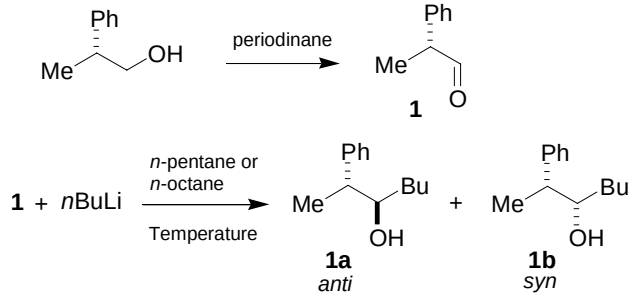

Scheme 1. The one step synthesis followed to prepare the chiral aldehyde **1** and the nucleophilic addition reaction conditions.

In all experiments the addition reaction was performed by introducing *n*BuLi into aldehyde **1** diluted in anhydrous *n*-pentane or *n*-octane at constant temperature (see supporting information). The temperature value was varied over a range of approx. 120 K. The reactions proceeded smoothly to give *anti* (**1a**) and *syn* (**1b**) alcohols (scheme 1). The diastereomeric ratio [*anti*]/[*syn*] was determined in each experiment by GC analysis of the corresponding trimethylsilylethers and results are reported as Supporting Information. The data for ln (*anti/syn)* versus 1/*T* were analyzed by a linear least-squares fitting to the Eyring equation and for each data set a residual analysis was applied to evaluate the number of linear

trends and to ascertain the presence of an inversion temperature. More specifically, the inversion temperature has been first estimated by fitting the complete $\{\ln S_i\ ,\ 1/T_i\ \}$ data set (ordered with increasing values of $1/T$) with a single regression line. The data pair corresponding to the largest absolute value residual has been used to partition the data set into left and right subsets, with the dividing point assigned to the left subset. The two groups of points have then been separately fitted with a least squares straight line. The intersection of these regression curves gives the estimated inversion temperature, while the differences $\Delta\Delta H^{\neq}$ and $\Delta\Delta S^{\neq}$ were obtained from the slopes and the intercepts of these linear plots (Table 1). The thermodynamic parameters are quite different in the two solvents. In particular in pentane, where little values of $\Delta\Delta H^{\neq}$ resulted, the differential activation entropy represents the main contribution to stereoselectivity.

			$T>T_{inv}$	$T<T_{inv}$	
Solvent	T_{inv} (K)	$\Delta\Delta H^{\neq}$ (kcal mol^{-1})	$\Delta\Delta S^{\neq}$ (cal mol^{-1}K^{-1})	$\Delta\Delta H^{\neq}$ (kcal mol^{-1})	$\Delta\Delta S^{\neq}$ (cal mol^{-1}K^{-1})
Pentane	204	-0.33 ± 0.06	+1.2 ± 0.2	+0.46 ± 0.14	+5.2 ± 0.7
Octane	288	-1.0 ± 0.1	-1.0 ± 0.4	-0.58 ± 0.04	+0.6 ± 0.2

Table 1. Differential activation parameters $\Delta\Delta H^{\neq}$, $\Delta\Delta S^{\neq}$ and inversion temperature T_{inv} for *n*BuLi addition to aldehyde **1** in *n*-pentane and *n*-octane as obtained from linear regression analysis of the experimental data.

The Eyring plots in figure 1 show the inverse temperature dependence of ln*S* to **1** in *n*-pentane and *n*-octane. Notwithstanding the little variation of the diastereomeric ratio [*anti*]/[*syn*] with *1/T*, the plots show for *n*-pentane an inversion temperature (T_{inv}) at 204 K, suggesting the presence of two different kinds of solute-solvent clusters: one above and one below T_{inv}. A similar behavior, although less evident, is observed using *n*-octane as the solvent, with the *anti* diastereoisomer being favored at all temperatures.

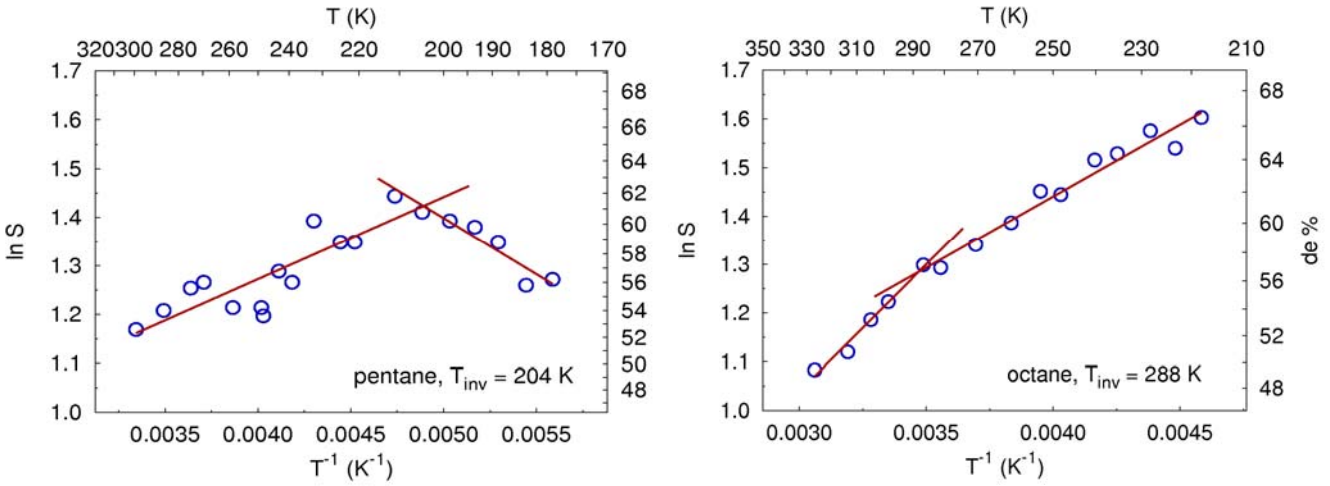

Figure 1. Eyring plots for the diastereomeric ratio obtained in the addition of *n*BuLi to aldehyde **1** in pure *n*-pentane (left) and *n*-octane (right). The two linear regression curves, obtained as described in the text, and the inversion temperature are shown together with the experimental results (circles).

COMPUTER SIMULATIONS

Our aim here is to investigate the existence of differences at molecular level in the solvation of the aldehyde in the two alkanes studied experimentally, via extensive molecular dynamics simulations at atomistic level [15, 16]. In practice, we have explicitly simulated (*R*)-2-phenyl-propionaldehyde in *n*-pentane and *n*-octane, examining the distribution of solvent molecules around the solute and the properties of the chiral solute in this explicit medium. To do this, we have described the *n*-alkane solvent with the NERD united-atoms Force Field (FF) [18] which was specifically developed for hydrocarbons, while the solute has been modeled by suitably modifying the OPLS-AMBER FF [19] by adding specifically derived point charges and by changing a torsional term. As the description of aldehyde torsion with respect to the bond CHO-C* is of fundamental importance in determining the conformations of the solute and the reaction products, we have performed first a preliminary test of the standard AMBER FF, by a comparison with quantum mechanical calculations at Hartree-Fock 6-31G* level [20] for the torsional potential. This has shown that the standard FF gives a description of the ϕ_1 torsion that is even qualitatively incorrect (figure 2) and, consequently, we have replaced the relevant AMBER FF parameters with new ones using the following procedure.

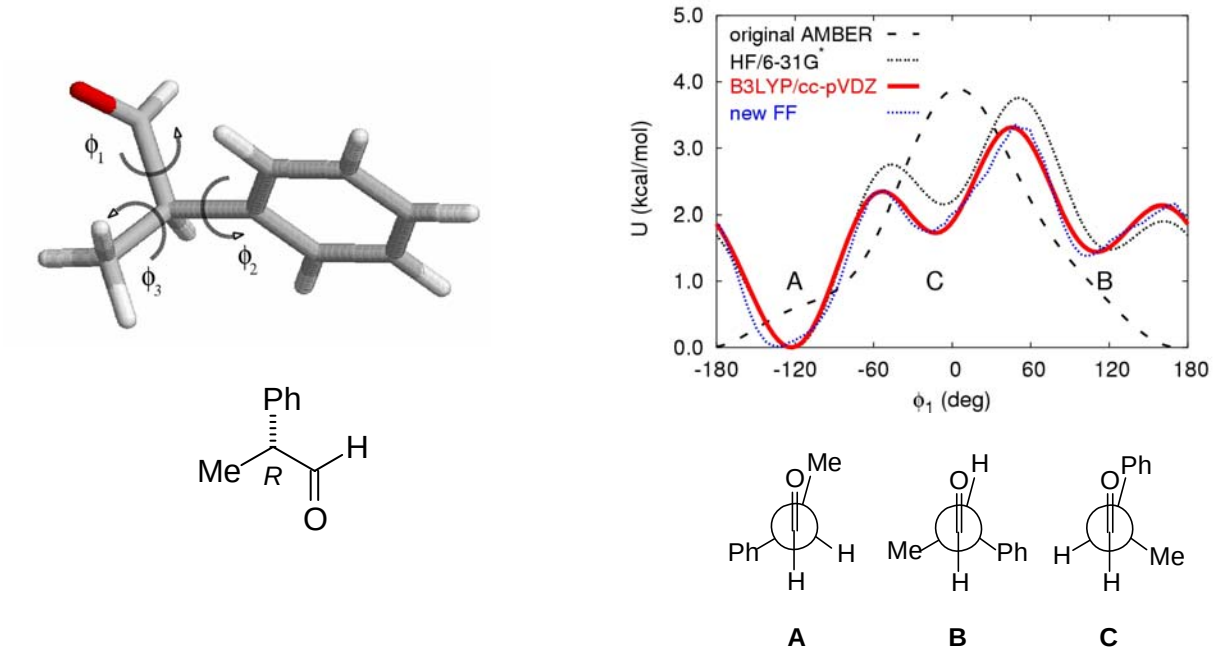

Figure 2. Definition of the torsional angles ϕ_i (left) and a plot of the torsional potential for the rotation around the CHO-C* bond (right) of (*R*)-2-phenyl-propionaldehyde as obtained from various levels of theory: original AMBER FF (black, long dashed), HF/6-31G* (black, short dashed), B3LYP/cc-pVDZ (red, thick line) used for parametrizing the new force field torsional term (blue dots, calculated in vacuum). The Newman projections of the minimal energy conformers are also shown.

The molecular geometry was optimized with the B3LYP density functional (DFT) using Dunning correlation consistent polarized valence double zeta (cc-pVDZ) basis set[20], and electrostatic-potential fitting atomic charges were also calculated and added to the force field. At the same level of theory, and for 24 conformations corresponding to uniformly spaced torsional angles in the range $-180^o < \phi_1 < 180^o$, the molecular structure was then relaxed while keeping fixed ϕ_1 at the desired value, thus obtaining a reference torsional energy profile (red curve in figure 2 and Table B in the Supporting Information). This overall DFT potential contains non-bonded contributions terms which in the AMBER type FF are given separately, and that have thus to be accounted for to avoid counting them twice in the simulation. In practice, the contribution $U_{nb}(\phi_1)$ of the non-bonded terms to the FF has been calculated from the logarithm of the "non-bonded" torsional angular distribution $P_{nb}(\phi_1)$ obtained from an MD simulation of an isolated molecule at 1000 K, in which the FF torsional potential was fixed to zero ($U_{nb}=-k_BT \ln P_{nb}$). The rationale of the method is that, at this high temperature, the conformations corresponding to all

angles are populated, and consequently a good conformational sampling can be achieved. The difference between the DFT and the nonbonded torsional potential has then been fitted with a truncated Fourier series expansion (six cosine and three sine terms) that has been used as the new FF torsional potential (see e.g. ref. [21]). We have verified the new force field torsional potential by two 600 ns simulations in vacuum at the temperatures of 270 and 320 K; the agreement with the original DFT potential is good (root mean square deviation: 0.14 kcal/mol) and the discrepancies are due to the limited number of Fourier series terms used in the force field for torsion ϕ_1.

The torsional potential obtained, which is in excellent agreement with recently published calculations and free jet millimeter-wave absorption spectroscopy experimental data [22], shows three minima corresponding to the preferred conformers. The most stable one, labeled A in figure 2, is the one with the carbonyl oxygen eclipsing the methyl group, while the conformer corresponding to the eclipsed hydrogen (B) is found to be less stable of about 1.4 kcal/mol and the conformer with the eclipsed phenyl (conformer C) has an energy 1.7 kcal/mol higher than conformer A.

We have performed MD simulations of samples composed of one solute: a (*R*)-2-phenyl-propionaldehyde molecule, and 50 surrounding solvent molecules using ORAC, a multiple time-step code developed by Procacci et al. [23]. This relatively small sample, contained in a periodic cubic box kept at atmospheric pressure, is sufficient to describe well the first solvation sphere and partially the second, as we have verified with additional simulations performed on larger samples containing 250 molecules of pentane at the temperature of 270 K and of octane at the temperature of 320 K (see figure 6). The temperature ranges, 170-270 K for *n*-pentane and 220-320 K for *n*-octane, have been chosen since they are sufficiently large to enclose the experimental inversion temperatures. The systems investigated required around 5 ns to equilibrate: a reasonable time [24] for a system composed of relatively simple molecules moving in low viscosity isotropic solvents [25]. Following the equilibration stage we have performed very long production runs of about 300 nanoseconds to get sufficiently good statistics. We have monitored the torsional angle ϕ_1 as function of time and verified that under these

conditions the sampling during the MD production runs is adequate to acquire statistically significant conformational population probabilities.

In view of assessing the molecular origin of the experimental diastereoselectivity, we have started comparing the conformational distributions around the CHO-C* bond (torsional angle ϕ_1) as computed from the MD trajectories for the pentane and octane solvents at the highest and lowest temperatures studied with the distributions calculated from a simulation of the aldehyde in vacuum (figure 3). We see that in both solvents the conformations of type A are more probable than in vacuum (i.e. are stabilized by the alkane); the conformations of type C and B are correspondingly destabilized, while the order of the conformational energies is preserved (A<B<C). The low temperature distributions (black curves) show that almost uniquely the conformation of type A is present in these thermodynamic conditions.

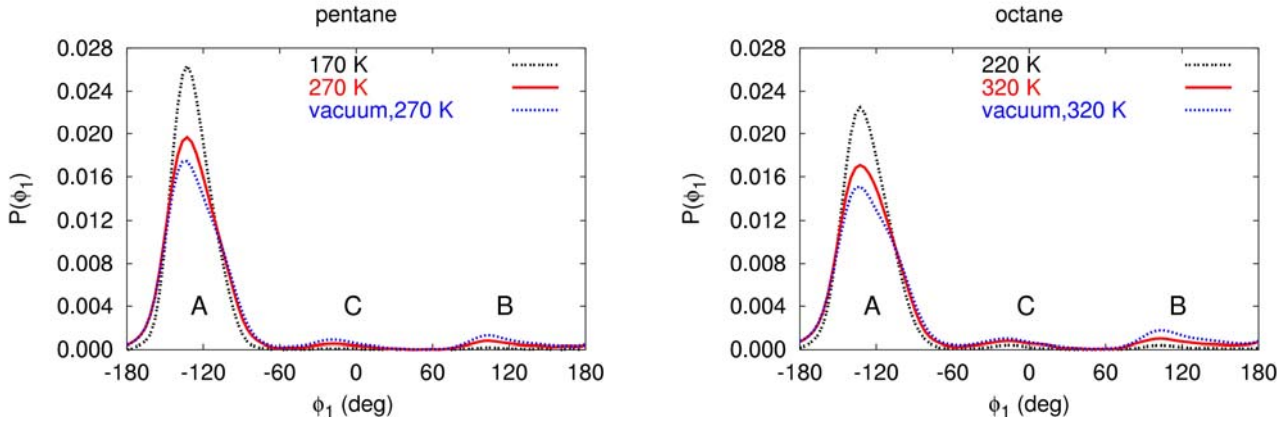

Figure 3: Normalized conformational distributions $P(\phi_1)$ in pentane (left) and octane (right) at the lowest (black) and highest (red) MD simulation temperatures, compared with the distribution obtained form a 600 ns MD NVT simulation of the aldehyde in vacuum at the highest temperature (B, blue).

To measure more quantitatively both solvent and temperature effects on the molecular structure, we have considered the mean squared angular fluctuations of the acyl, methyl and phenyl groups (figure 4), that have been computed as the average $<(\Delta\phi_i)^2>$ at coarse grained intervals Δt of one picosecond for each temperature. Not surprisingly, the mean squared fluctuations increase linearly with temperature and their slopes provide an estimate of a local "torsional diffusion coefficient". However an evident jump in the curves is observed when changing solvent from pentane to octane (at 220 K): this is again

consistent with a change in the local mobility due to a modification in solvation, with octane allowing larger conformational fluctuations of the substrate than pentane.

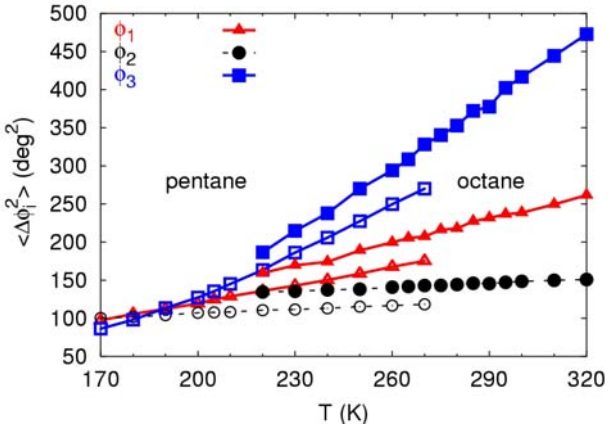

Figure 4: Mean squared angular fluctuations $<(\Delta\phi_i)^2>$ in pentane (left, 170-270 K) and octane (right, 220-320 K) solutions, calculated for rotations of the acyl (ϕ_1, squares), methyl (ϕ_2, circles) and phenyl (ϕ_3, boxes) groups.

Having verified that solvent effects are present, we have examined if our data support the existence of an inversion temperature, in particular trying to identify some indicators connected to changes in solvation with temperature that can on one hand be obtained from the MD simulations, and on the other be related to the diastereoselectivity.

We start by examining the solvent structuring around the carbonyl through one of the many atom-atom radial distribution functions that can be defined. In particular, we calculate the distribution $g_0(r)$ of the distances between the carbonyl carbon taken at the center and each of the united atoms belonging to solvent molecules (see figure 5), sampled on a spherical region:

$$g_0(r) = \frac{1}{4\pi r^2 \rho}\left\langle \delta\left(r - r_{ij}\right)\right\rangle_{ij}, \qquad (2)$$

where r_{ij} is the carbon-solvent distance and $\rho=N/V$ is the number density.

The results for $g_0(r)$ are plotted in figure 5. We see a local structuring of the solvent, more pronounced in pentane than in octane, where the first and second peak of $g_0(r)$ are actually quite similar; as already mentioned, we notice that the samples sizes we have used are sufficient to allow for the formation of

two solvation spheres. Test runs on larger samples with N=250 solvent molecules show that no further relevant structuring occurs as the bulk limiting value $g_0(r)=1$ is obtained.

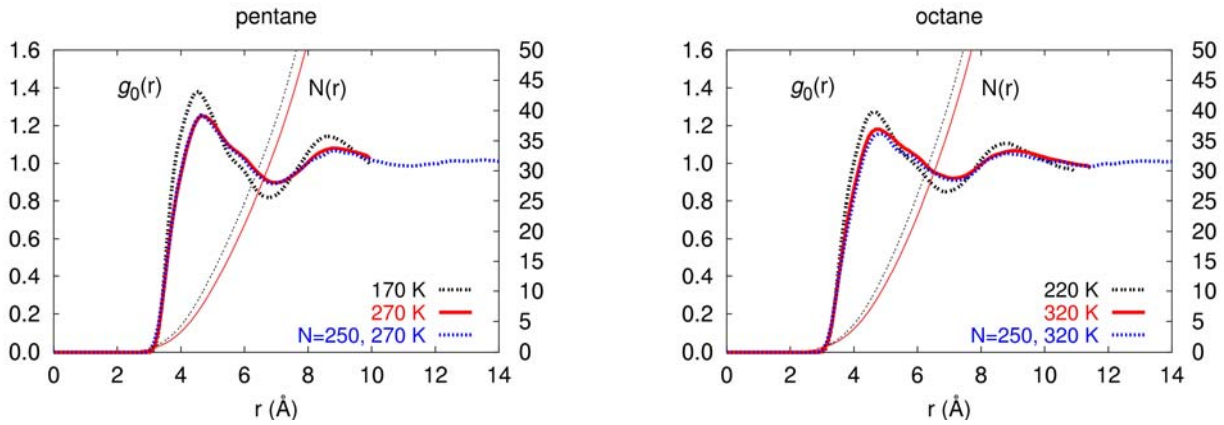

Figure 5: The radial distribution function $g_0(r)$ around the carbonylic carbon and the average number of CH_n centers $N(r)$ in pentane and octane calculated from the highest and lowest temperature MD simulation trajectories. We also show the radial distribution function calculated from simulations of a larger sample with 250 solvent molecules (blue dotted lines).

Regarding the effect of temperature, we notice that an increase of temperature of 100 K, from well below to well above the experimentally observed inversion temperature, broadens the peaks of $g_0(r)$, but is not sufficient to modify the extent of the local, short range order. In addition, for both solvents the shape of the radial distribution changes very little in the simulated temperature interval.

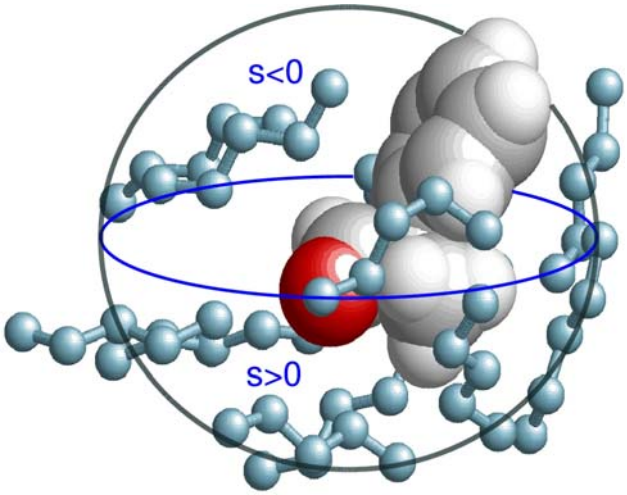

Figure 6: Snapshot of the united atom pentane molecules partially or totally contained in the first solvation sphere around the carbonyl carbon (pentane, 180 K) with the definition of positive and negative faces of the carbonyl. Solvent atoms have been rendered 5 times smaller than the actual size to increase visibility.

Since the standard radial distribution depends only on distance it cannot be used to discriminate between atoms above or below the aldehyde plane. Thus, in order to try to quantify the facial selectivity of solvation, we have modified this indicator by defining a specific parameter $s = (\mathbf{n} \cdot \mathbf{r}_{ij}) / |\mathbf{n} \cdot \mathbf{r}_{ij}|$, where **n** is the normal to the plane identified by the three atoms of the acyl group. This plane is defined so that s is positive on the face of the π carbonyl bond leading under nucleophilic attack to an *anti* product, and negative on the other face (see figure 6).

We have then distinguished the two contributions to the total radial distribution function according the sign of s and computed the density distribution $g_0(sr)$ around the two faces:

$$g_0(sr) = \frac{1}{2\pi r^2 \rho} \left\langle s\delta(r - r_{ij}) \right\rangle_{ij} . \qquad (3)$$

These $g_0(sr)$ curves (figure 7) show clearly that the solvation is strongly facial selective, with the positive side being on average more populated than the negative one at every temperature studied. It is also possible to introduce a solvation radius for each face of the π bond, defined as the position of the first minimum of the distribution function: the ratio of these distances is solvent dependent and changes with temperature, as shown in figure 8. We find that the solvation radius measured for the positive face (empty and filled red squares) is always smaller than one measured for the negative face (empty and filled blue circles), in spite of the former region being more populated: we see that the solvation is strongly face-selective and the positive face is surrounded by a more structured solvent cage. All radii plotted in figure 8 show some discontinuity in their temperature dependence: in principle this might be related to the experimental inversion temperatures, but we have found these data not sensitive enough to be used for a recovery of the experimental result. The number of united atoms centers $N(sr)$ for the two faces does not change significantly with temperature (figures 5 and 7), and the positive face is always more solvated: this is reflected in the experimental outcome that the *anti* product is favored at all temperatures.

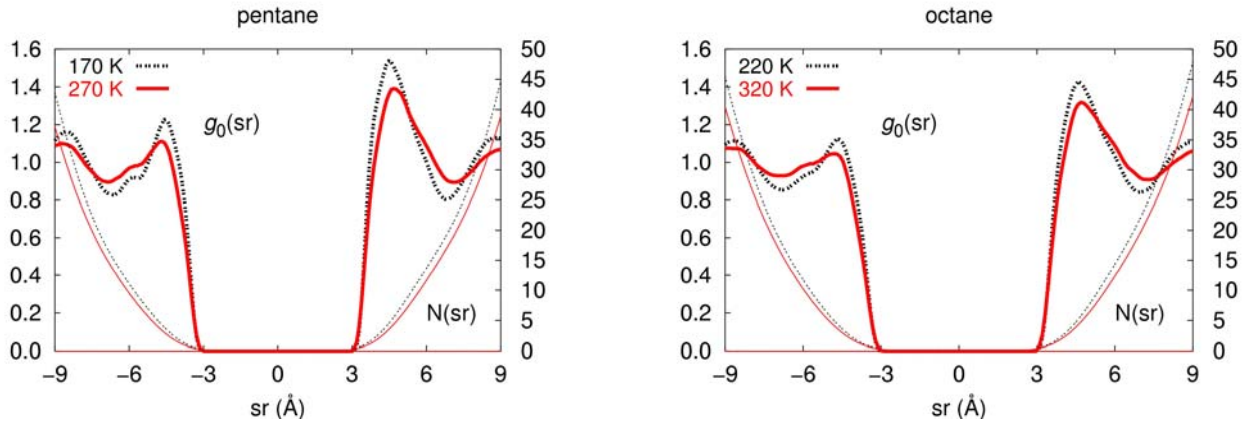

Figure 7: The face-dependent radial distribution function $g_0(sr)$ around the carbonylic carbon and the corresponding number N(sr) of CH_n groups contained in each hemispherical region.

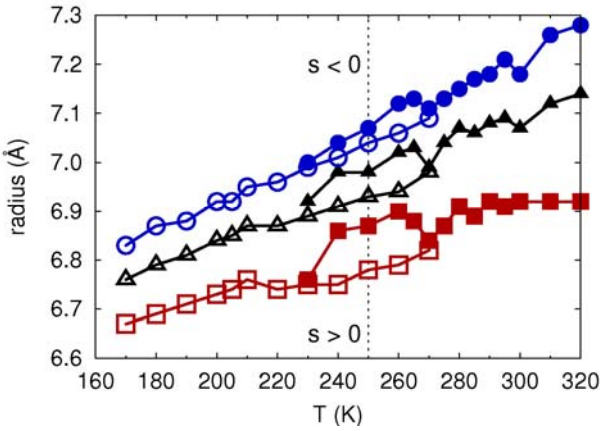

Figure 8: Radii of the first solvation shell for the carbonyl carbon of the aldehyde in pentane (empty symbols) and octane (filled symbols), as estimated from the $g_0(sr)$ distribution: face independent (black triangles), positive face (red squares), and negative face values (blue circles).

We are still left with problem of finding an observable that is sensitive enough to changes in solute solvation as a function of temperature. Since it has been demonstrated experimentally by CD studies of the solvated aldehyde [14] that the inversion temperatures are directly connected to dynamic solute-solvent clustering effects, and since it is reasonable to suppose that the diasteroselectivity might depend on the degree of chirality of the chiral reactant, we have examined as a candidate indicator of selectivity change the average chirality of (*R*)-2-phenyl propionaldehyde, as a function of temperature and solvent nature. There are of course many quantitative estimators of molecular chirality, based on different

operational definitions of chirality [26, 27, 28] or on the choice of different molecular observables (for a recent review see [29]). Here we are not concerned with spectroscopic properties like CD itself or optical rotation, but rather with an indicator of the effective (conformationally averaged) chirality in molecular shape as relevant to solute-solvent interactions. Thus we have chosen to calculate a chiral index that has already been successfully used in tackling problems connected with effects of solute chirality, particularly in theoretical studies of helical twisting power, i.e. of the effectiveness of a chiral solute in generating a twisted (cholesteric) phase when dissolved in a nematic solvent [30, 31]. This molecular chirality index can be written, as described in detail in [30] as:

$$G_{0S} = 4!/(3N^4)\sum_{\{ijkl\}} \hat{P}_{ijkl}\left\{m_i m_j m_k m_l \left\{\left[(\mathbf{r}_{ij}\times\mathbf{r}_{kl})\cdot\mathbf{r}_{il}\right](\mathbf{r}_{ij}\cdot\mathbf{r}_{jk})(\mathbf{r}_{jk}\cdot\mathbf{r}_{kl})\right\}/\left[(r_{ij}r_{jk}r_{kl})^2 r_{il}\right]\right\}, \qquad (4)$$

where $\mathbf{r_{ij}} = \mathbf{r}_i - \mathbf{r}_j$ is an interatomic vector and $\mathbf{r}_i$, m_i the position and mass in atomic units of the i-th atom. The summation is performed over all different sets of four atoms $\{ijkl\}$ out of the N atoms in the molecule, while $\hat{P}_{ijkl}\{A_{ijk}\}$ is an operator generating a sum over all the permutations of i, j, k, l . The index G_{0S} assigns to each observed molecular conformation a measure of chirality obtained as a mass-weighted degree of asymmetry of the atomic coordinates, with a sign that can be used for a right/left classification [26,27]. We report in figure 9 the logarithm of the conformationally averaged value of $\langle G_{0S}\rangle$ obtained from simulation trajectories. We see that the conformationally averaged solute chirality decreases with T, and that it is systematically higher in pentane than in octane (possibly an effect of temperature). In figure 9 we also see a clear evidence of two regions with distinct chiral index vs temperature slopes. From these results a break temperature (named T_{CI}) can be determined with the same algorithm described in the experimental section. It is gratifying to see that the break temperatures obtained (223 K in pentane and 274 K in octane) are close to the inversion temperatures derived from the Eyring plots of the experimental diastereoselectivity (see figure1). On the other hand there is no reason to believe that only solvation effects directly connected to chirality are the only enthalpic effects that can contribute to the reaction outcome and this is probably the origin of the differences between the slopes of the $\langle G_{0S}\rangle$ and selectivity curves. On the whole our findings definitely supports the hypothesis

that the inversion temperature for the stereoselective reaction studied is largely solvent-driven and that the chiral index $<G_{0S}>$ is a useful monitor of these solvation changes.

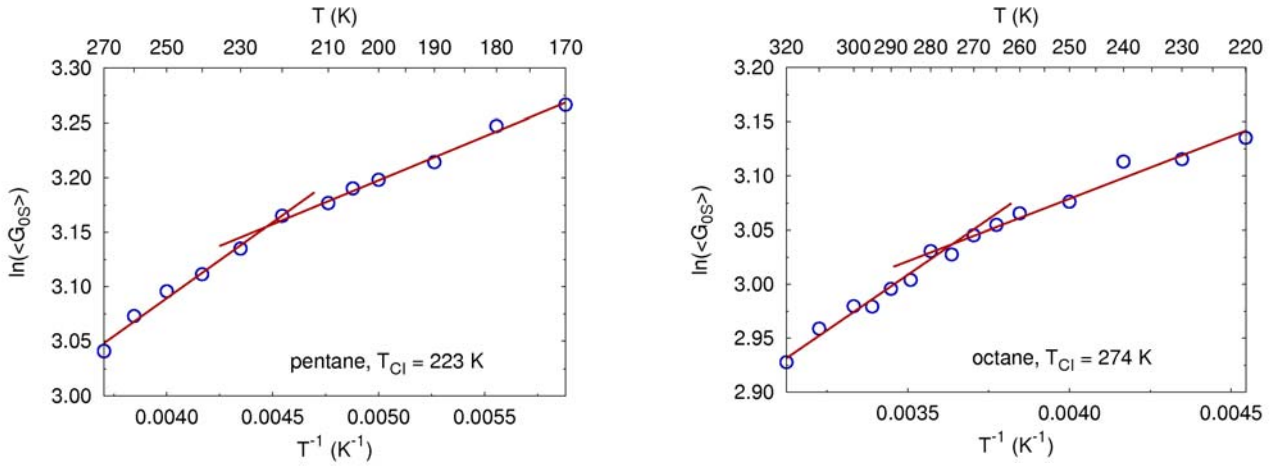

Figure 9: The logarithm of the average molecular chiral index $<G_{0S}>$ for (*R*)-2-phenyl-propionaldehyde dissolved in pentane (left) and octane (right) as obtained from the MD simulations (circles) together with the regression lines and the chiral break temperatures T_{CI}.

CONCLUSIONS

The molecular level description of solvation processes and of their effects on the details of chemical reactions is an important topic that still has a large margin for development, both from the point of view of understanding and rationalization and, even more, from that of predicting temperature dependent effects like inversion temperatures [7,8]. Here we have approached the specific case of stereoselectivity in a nucleophilic addition, with the aim of verifying the hypothesis [12] that the observed solvent and temperature effects on facial selectivity are closely related to the nature of solvation in the local microenvironment surrounding solute molecules.

We have performed stereoselectivity experiments for (*R*)-2-phenyl-propionaldehyde in two quite similar solvents: pentane and octane at a number of temperatures and found (i) that they show an inversion temperature and (ii) that these temperatures are quite different (204 and 288K). We have then performed

extensive molecular dynamics computer simulations for the two aldehyde-solvent systems and measured the facial solvation of the carbonyl bond. We have found that the close presence of a chiral center determines different average solvent densities on the two faces of the π-bond and that the density depends on the solvent used; from this point of view, pentane and octane show remarkable differences, which are likely to affect the diastereoselectivity of a nucleophilic reaction if we think at the solvent density as a measure of accessibility of a face. The higher diastereoselectivity reported in pentane can be rationalized as an higher accessibility of the face which leads to the *anti* product. This concept is not sufficient in itself to explain the presence of an inversion temperature, and the quantification from our simulations of the amount of solvent in the neighborhood of a side of the carbonylic bond has proven to be not sufficiently sensitive for the purpose. We have then focused on a solute physical property, the conformationally averaged molecular chiral index [30,31] $\langle G_{0S} \rangle$, that we have determined from the simulations. We have found that $\ln\langle G_{0S} \rangle$ exhibits a nonlinear temperature dependence in both solvents with chirality break temperatures T_{CI} which are in a good agreement with the experimental selectivity inversion temperatures (pentane: T_{CI}=223 K, T_{inv}=204 K; octane T_{CI}=274 K, T_{inv}=288 K). The MD simulations thus show the existence of an inversion temperature which can be ascribed to the interaction of the aldehyde with the solvent and it is, in this respect, independent on the nature of the reactant. The chiral index $\langle G_{0S} \rangle$ hence results in a sensitive probe for temperature and solvent effects.

Although the detailed nature of the specific solvent-solute interactions responsible for the inversion of selectivity still has to be investigated in general terms, we believe that the approach developed here, with full inclusion of the solvent, provides an important opening and warrants a systematic study on a larger class of solvents and reactions.

ACKNOWLEDGMENTS

We gratefully acknowledge financial support from MIUR through FIRB project "*Solvent and temperature effect on stereoselective processes in organic synthesis*", from University of Bologna and from INSTM.

SUPPORTING INFORMATION

1. **Experimental part**.
2. **Table A.** Percentage concentration of *anti* and *syn* diastereoisomers in the *n*BuLi addition to aldehyde **1** in *n*-pentane and *n*-octane.
3. **Table B.** Fit parameters of the DFT torsional potential.

REFERENCES

[1] Reichardt, C. *Solvents and Solvent Effects in Organic Chemistry*; 3rd ed., Wiley-VCH: Weinheim, 2003.

[2] For recent examples see for instance: (a) Roland, S.; Mangeney, P. *Eur. J. Org. Chem.* **2000**, 611; (b) Cainelli, G.; Giacomini, D.; Galletti, P. *Eur. J. Org. Chem.* **1999**, 61. (c) Crimmins, M. T.; Choy A. L.; *J. Am. Chem. Soc.* **1997**, *119*, 10237. (d) Murray, R. W.; Singh, M.; Williams, B. L.; Moncrieff, H. M.; *Tetrahedron Lett.* **1995**, *36*, 2437. (e) Saito, T.; Kawamura, M.; Nishimura, J. *Tetrahedron Lett.* **1997**, *38*, 8231. (f) Wipf, P.; Jung, J-K. *Angew. Chem., Int. Ed. Engl.* **1997**, *36*, 764. (g) Denmark, S. E.; Nakajima, N.; Nicaise, O. J-C. *J. Am. Chem. Soc.* **1994**, *116*, 8797. (h) Reetz, M. T.; Stanchev, S.; Haning, H. *Tetrahedron* **1992**, *48*, 6813.

[3] Cram, D.; Kopecky, K. *J. Am. Chem. Soc.* **1952**, *74*, 5828.

[4] Cherest, M.; Felkin, H.; Prudent, N. *Tetrahedron Lett.* **1968**, 2199.

[5] Ahn, N.T.; Eisenstein, O. *Nouv. J. Chem.* **1977**, *1*, 61.

[6] (a) Eyring, H. *J. Phys. Chem.* **1935**, *3* , 107. (b) Glasstone, S.; Laidler, K. J.; Eyring, H. *The Theory of Rate Processes.* McGraw-Hill: New York, 1941, chapter 4.

[7] For a review see: Buschmann, H.; Scharf, H.-D.; Hoffmann, N.; Esser, P. *Angew. Chem.* **1991**, *103*, 480; *Angew. Chem., Int. Ed. Engl.* **1991**, *30*, 477.

[8] (a) Cainelli, G.; Giacomini, D.; Galletti, P. *Chem. Commun.* **1999**, 567; (b) Cainelli, G.; Giacomini, D.; Galletti, P.; Marini, A. *Angew. Chem.* **1996**, *108*, 3016, *Angew. Chem. Int. Ed. Engl*. **1996** , *35*, 2849.

[9] (a) Fleischer, J. M.; Gushurst, A. J.; Jorgensen, W. L. *J. Org. Chem*. **1995**, *60*, 490; (b) Tomoda, S.; Senju, T. *Chem. Commun.* **1999**, 621.

[10] Sicinska, D.; Paneth, P.; Truhlar, D. G. *J. Phys. Chem. B* **2002**, *106*, 2708.

[11] see, e.g., Cramer, C. *Essentials of Computational Chemistry* ; Wiley: Chichester, 2002.

[12] Cainelli, G.; Giacomini, D.; Galletti, P.; Orioli, P. *Angew. Chem. Int. Ed. Engl.* **2000**, 39, 523.

[13] Cainelli, G.; Giacomini, D.; Galletti, P.; Orioli, P. *Eur. J. Org. Chem.*, **2001**, 4509.

[14] Cainelli, G.; Galletti, P.; Pieraccini, S.; Quintavalla, A.; Giacomini, D.; Spada, G. P. *Chirality*, **2004**, *16*, 50.

[15] Frenkel D.; Smit, B. *Understanding Molecular Simulations: From Algorithms to Applications;* Academic Press: San Diego, 1996.

[16] Pasini, P.; Zannoni, C., Eds. *Advances in the computer simulations of liquid crystals*; Kluwer: Dordrecht, 2000.

[17] Botuha, C.; Haddad, M.; Larchevêque, M. *Tetrahedron: Asymmetry* **1998**, *9*, 1929.

[18] Nath, S.K.; Escobedo, F.A.; de Pablo, J. J. *J. Chem. Phys.* **1998**, *108* , 9905.

[19] Cornell, W. D.; Cieplak, P.; Bayly, C. I.; Gould, I. R.; Merz, K. M., Jr.; Ferguson, D. M.; Spellmeyer, D. C.; Fox, T.; Caldwell, J. W.; Kollman, P. A. *J. Am. Chem. Soc*. **1995**, *117*, 5179.

[20] Koch, W.; Holthausen, M. C. *A Chemist's Guide to Density Functional Theory*, Wiley-VCH Verlag GmbH: Weinheim, 2001.

[21] Earl, D. J.; Wilson, M. R. *J. Chem. Phys.* **2003**, *119*, 10280.

[22] Maris, A.; Caminati, W. *Phys. Chem. Chem. Phys.* **2003**, *5,* 2795.

[23] Procacci, P.; Paci, E.; Darden, T.; Marchi, M. *J. Comput. Chem.* **1997**, *18*, 1848.

[24] Berardi, R.; Muccioli, L.; Zannoni, C. *ChemPhysChem* **2004**, *5*, 104

[25] see, e.g., Dorfmüller,Th.; Pecora, R. *Rotational dynamics of small and macromolecules*; Springer-Verlag: Berlin, 1987.

[26] Ruch, E.; Runge, W.; Kresze, G. *Angew. Chem., Int. Ed. Engl* **1973,** *20,* 12

[27] Ruch, E., *Angew. Chem., Int. Ed. Engl* **1977,** *65,* 16

[28] Buda, A.; Mislow, K., *J. Am. Chem. Soc.* **1992**, *114*, 6006.

[29] Petitjean, M., *Entropy* **2003**, *5*, 271.

[30] Solymosi, M.; Low, R.J.; Grayson, M.; Neal, M. P. *J. Chem. Phys.* **2002**, *116*, 9875.

[31] Neal, M. P.; Solymosi, M.; Wilson, M. R.; Earl, D. J. *J. Chem. Phys*. **2003**, *119*, 3567.